Dynamic Laminate Model for Broadband Frequency Prediction

Gérard BORELLO[1], Arnaud DUVAL[2]

[1] InterAC, France

[2] Faurecia, France

ABSTRACT

Orthotropic multi-layered panels are well-spread in transport industry. Specific methods of prediction need to be addressed depending on construction. Laminate models based on zig-zag theory are useful for aircraft fuselage prediction and more generally for composite panels. As soon as a very soft layer is inserted between stiff layers, breathing modes are occurring in mid and high frequencies and assumed zig-zag displacement field is no more representative of the actual behavior. It has to be replaced by 3D FEM modeling increasing cost of calculation. In Statistical Energy Analysis (SEA) models, because of the extended calculation range, the 'classical' laminate equations are limiting the class of simulated systems and zig-zag theory is most often pushed outside its natural limits. A new multi-scaled dynamic laminate model has thus been developed to take into account transverse decoupling of layers while converging correctly to equivalent static plate at low frequency. This laminate model accepts any kind of mechanical orthotropic layers as well as thin 2D acoustic layers. They may be ribbed or not to increase stiffness. Damping loss factor of the assembly is predicted from internal damping of the various layers. Basic equations will be presented as well as some early validation work.

Keywords: SEA, Laminate, Structural Dynamics I-INCE Classification of Subjects Number(s): 47.3

1. INTRODUCTION

For fast modeling of complex multi-layered plate-like floors or curved composite sandwich panels, dedicated analytical Dynamic Laminate theory has been developed and implemented in SEA+ software based on SEA for overcoming limitations experienced in FEM solvers.

The mean Damping Loss Factor (DLF), the modal density and the wavenumber of laminate plates and shells are then predicted from properties of individual layers over a broadband frequency range. This theory is multi-scaled as it supports motion transition from global panel modes at low frequency to local modes of individual layers above first transverse resonance frequencies (along normal axis to plate). The actual 3D dynamical behavior of the system is described by a set of 2D inter-coupled thin layers. Each layer may oscillate at high frequency on its uncoupled degrees of freedom i.e. displacement in x, y, z directions. The theory is validated against FEM calculations and measurements. [7] provides the necessary background to composite simulation and [6] is reviewing all general formulations. General motivation about proposed theory has been initiated in [5].

2. COUPLING GLOBAL AND LOCAL DISPLACEMENTS

Modeled systems are composed of flat or curved contiguous-panel layup with constant thickness per panel as shown in Figure 1. If any curvature, related radius is assumed to be the same for all layers. Retained degrees of freedom are motions (u, v, w) of layers at their neutral fiber resp. in the x, y, z directions, expressed as sum of two displacements:

- a global displacement (u_0, v_0, w_0) expressed at the neutral fiber of which elastic coefficients provided by Hooke's Law, are computed assuming static bending, shear or extension and integrated over the total thickness of the layup;
- a local relative displacement of each layer (u_i, v_i, w_i) expressed at the individual neutral fiber of each layer.

[1] gerard.borello@interac.fr

[2] arnaud.duval@faurecia.com

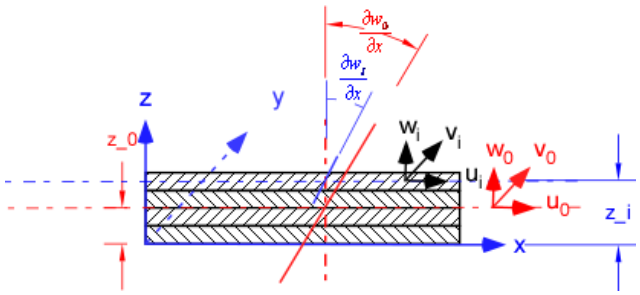

Figure 1 - Degree of freedom of the laminate assembly

The absolute displacement of a specific layer is then the sum of global and relative displacements:

$$\vec{w}_i = \vec{w}_0 + \vec{w}_{Ri} = (u_0, v_0, w_0) + (u_{Ri}, v_{Ri}, w_{Ri}).$$

Vertical direction vibration is given by the absolute displacements of the various neutral fibers. A common-to-all layers space function *g(x,y)*, describes the displacement field along x and y coordinates. It then gives:

$$\vec{w}_i(x, y, z) = g(x, y)\{(U_0, V_0, W_0) + (U_{Ri}, V_{Ri}, W_{Ri})\}$$

where (U_0, V_0, W_0) represents the low frequency equivalent plate global amplitudes and (U_{Ri}, V_{Ri}, W_{Ri}) the local relative ones for a given *i*-layer in the coupled dynamics of the assembly.

The uncoupled dynamics of *i*-layer is described by its orthotropic dynamic stiffness and mass operators L_i and M_i which are defined in the principal axis of orthotropy as follows:

$$L_i = \begin{bmatrix} C_{11}\partial^{"}_{x^2} + C_{66}\partial^{"}_{y^2} & (C_{12} + C_{66})\partial^{"}_{xy} & 0 \\ (C_{12} + C_{66})\partial^{"}_{xy} & C_{66}\partial^{"}_{x^2} + C_{22}\partial^{"}_{y^2} & 0 \\ 0 & 0 & D_{11}\partial^{(4)}_{x^4} + D_{22}\partial^{(4)}_{y^4} + 2(D_{12} + 2D_{66})\partial^{(4)}_{x^2y^2} \end{bmatrix}, \quad M_i = \rho_i t_i \begin{bmatrix} \partial^{"}_{t^2} \\ \partial^{"}_{t^2} \\ -\partial^{"}_{t^2} \end{bmatrix} I$$

where *I* is the identity matrix and C_{lk}, D_{lk} the elastic parameters. L_i is then rotated in the global *(x, y)* plane before any use in the dynamic matrix of the layup. Similarly, $\vec{w}_0$ is described by L_0 and M_0. Because of the non-null virtual work of $\vec{w}_{Ri}$ in the force field due to $\vec{w}_0$, L_i and L_0 are cross-coupled by the operator L_{0R} as well as M_i and M_0 by M_{0R}.

The coefficients l_{kl} of L_{0R} are obtained by first expressing the Lagrangian related to total kinetic and potential energies using virtual work principle and then by applying Euler-Lagrange's equations to get the equilibrium equations.

For example, the total kinetic energy T_z per unit m² summed-up in *z*-direction is related to the kinetic energy T_{iz} of individual *i*-layer by herebelow relationship:

$$\mathbf{T}_{iz} = \frac{1}{2}\int_{x,y}\int_{z\in\{z_i - t_i/2, z_i + t_i/2\}} \rho_k(z)\dot{w}^2 dz dx dy = \int_{x,y}\int_{z} \rho_k(z)\left[\dot{w}_0 + \dot{w}_{Ri}\delta(z - z_i)\right]^2 dz dx dy$$

$$T_{iz}(\text{per m}^2) = \frac{1}{2}\rho_0 t_i \dot{w}_0^2 + \frac{1}{2}\sum_i \rho_i t_i \dot{w}_{1i}^2 + \sum_i \rho_i t_i \dot{w}_{Ri}\dot{w}_0 \qquad T_z = \sum_{i=0,N} T_{iz}$$

with t_i thickness of *i*-layer. From T_z expression are deduced the coefficients m_{0i} of M_{0R} which couple w_0 and w_{Ri}: $m_{0i} = \rho_i t_i$.

The potential energy coupling global and local degrees of freedom is not so easy to derive. Example of calculation is given for the coupling terms related to bending energy carried by w_0 to w_i.

$\sigma_{0x} + \sigma_{1ix}$ and $\varepsilon_{0xx} + \varepsilon_{1ix}$ are respectively the absolute extensional stress and strain exerted in the local layer by the global bending. The total potential bending energy is obtained by integrating the work $\sigma\varepsilon$ along *z*. We see from next result (integrated along *x* direction only for simplification) that each local layer is working in the displacement field of global 0-layer, creating coupling between

second derivative of displacements $\frac{\partial^2 w_0}{\partial x^2}$ and w_i.

$$\mathbf{U}_{zi} = \frac{1}{2}\int_x \int_{z\in\{z_i - t_i/2, z_i + t_i/2\}} [\sigma_{0x} + \sigma_{Rix}][\varepsilon_{0xx} + \varepsilon_{Rix}] \cdot dz dx = \frac{1}{2}\int_{z\in\{z_i - t_i/2, z_i + t_i/2\}} \left[\tau_{00(i)} + \tau_{RiRi} + \tau_{0Ri}\right] dz = \frac{1}{2}\int_x \tau_{iz}(x) dx$$

$$\tau_{iz}(x) = \frac{1}{2} g(x) \left\{ E_0 \left[d_i^2 t_i + \frac{t_i^3}{12} \right] W_{0x^2}^{"2} + E_{1i} \frac{t_i^3}{12} W_{1ix^2}^{"2} + \left[E_0 + E_{1i}\right] \frac{t_i^3}{12} W_{0x^2}^{"} W_{1ix^2}^{"} \right\}$$

d_i are distances between i-layer neutral fibers and global neutral axis of the assembly. $g(x)$ is the assumed wave function along x.

Coupling bending energy to in-plane energy and in-plane energy to in-plane energy is performed in a similar way providing at the end all coefficients to fill M_{0R} and L_{0R} coupling operators.

3. COUPLING RELATIVE DISPLACEMENTS

Individual layers are mutually excited both side of their boundary surfaces. As chosen motion variables are not continuous along z but only defined at neutral fibers, the coupling along z is described in term of coupling impedances by spring-like relationships.

To avoid redundancy in degrees of freedom, the relative displacement is thus taken as the blocked displacement of one layer when the others are clamped. For example, if three layers are coupled (see Figure 2) with blocked neutral fibers of the two extreme ones, the displacement of the mid layer neutral fiber in z-direction is generating a compression field and the related compression energy U can be estimated from the compression impedance K_{zz}.

Assuming a linear compression strain continuous at interfaces A and B, potential energy is thus given by:

$$U = \frac{1}{2}\left\{ K_{zz-} \left(w_k - w_{k-1} \right)^2 + K_{zz+} \left(w_k - w_{k+i} \right)^2 \right\}$$

and K_{zz} both sides of i-layer by:

$$K_{zz-} = \frac{K_{zz}^{(k-1)} K_{zz}^{(k)}}{K_{zz}^{(k-1)} + K_{zz}^{(k)}} \qquad K_{zz+} = \frac{K_{zz}^{(k+1)} K_{zz}^{(k)}}{K_{zz}^{(k+1)} + K_{zz}^{(k)}} \qquad K_{zz}^{(k)} = \beta E_k / t_k$$

The parameter β is depending on $g(x,y)$ function as K_{zz} is a stiffness per unit m², proportional to $\frac{1}{A}\int_{x,y} g(x,y)$. More generally all stiffness's generated by stress components on upper and lower (x,y) boundaries are proportional to β.

Calculation of inter-forces between adjacent layers is extended to shear and bending-to-shear coupling and provides the necessary additional coupling terms between local layers in matrices K_{RiRj}. Four interactions between adjacent layers are taken into account. Compression along z through K_{zz}, boundary in-plane shear through K_{xy}, transverse section shear through K_{zs} and a more subtle force coupling rotation of transverse section of one layer to the in-plane shear in the adjacent layer, through K_{ws}.

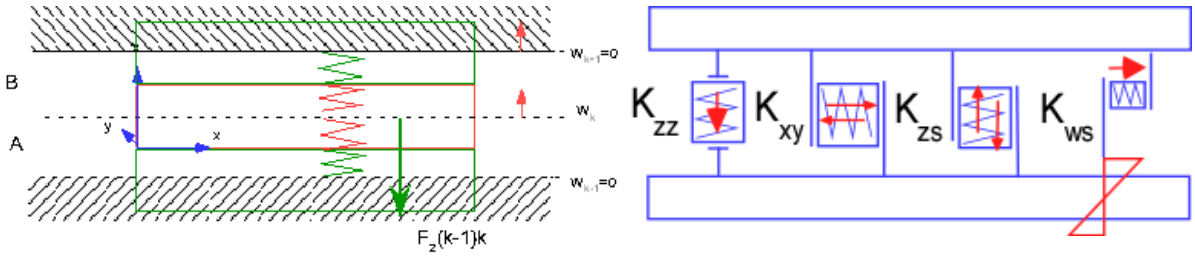

Figure 2 - Left, Sketch for z-stiffness term derivation of K_{zz} impedance and right the four coupling impedances introduced in the laminate model

4. MASS AND STIFFNESS MATRICES OF THE ASSEMBLY

The full analytical mass and stiffness matrix operator is built from the M_i, M_{0i}, L_0, L_i L_{0Ri} and K_{RiRj}. Figure 3 shows the structure of the resulting linear equations.

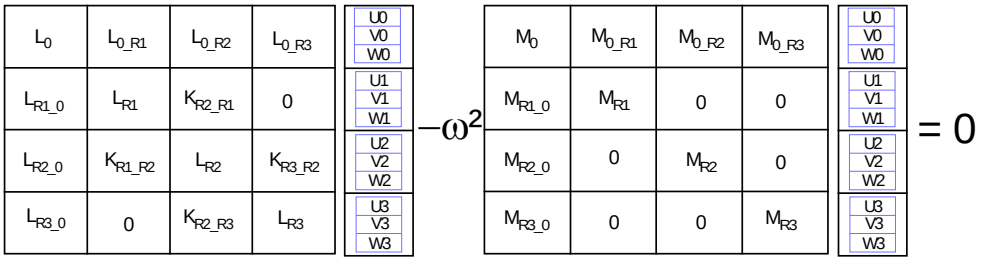

Figure 3 - The pattern of dynamic equations for 3 coupled layers

To get a fast analytical solution, displacements in the (*x*,*y*) plane are constrained to $g(x,y) = \sin\frac{m\pi x}{L_x}\sin\frac{n\pi y}{L_y}$ in case of simply supported edges at boundary.

When applying the differential operators to *g(x,y)*, *L* and *K* matrices are becoming functions of quantic *m* and *n* numbers. For each pair (*m*,*n*), an eigenvalue problem is solved, leading for N assembled layers system to 3x(N+1) eigenvalues, λ_{imn}. After extraction, λ_{imn} are sorted into extensional, shear and bending categories analyzing the relative importance of eigenvector amplitudes in each *u, v, w* directions.

Finally, the band-averaged modal densities and the band-averaged wavenumbers are estimated from the set of all discrete λ_{imn} up to some maximal *m*, *n* orders limited by the upper frequency of calculation.

The model is made more general by introducing frequency-dependent elastic parameters.

To estimate the mean DLF of the assembly, *L* and *K* matrices are made complex. For this, Young's and shear moduli of *i*-layers are multiplied by $(1+j\eta_i)$ at the related frequency.

The eigenvalue equation with frequency-dependent elastic coefficients is transformed into equation:

$$\tilde{L}(\omega) - \omega^2 M = 0$$

An approximate solution is found in two iterations:

- *L* matrix is made real and problem $\mathrm{Re}\left\{\tilde{L}(\omega=\omega_0)\right\} - \omega^2 M = 0$ is solved (classical eigenvalue problem) for a given set of (*m*, *n*) where $L(\omega_0)$ is the dynamic matrix at first defined frequency of elastic coefficient spectra. Solutions are the real set of eigenvalues $\left\{\lambda_0^{(m,n)}, \lambda_1^{(m,n)}, .., \lambda_k^{(m,n)}\right\}$.

For same *m*, *n* values, stiffness matrix is then taken equal to: $\tilde{L}\left(\omega=\sqrt{\lambda_0^{m,n)}}\right)$. The eigenvalue problem $\tilde{L}(\sqrt{\lambda_0^{m,n)}}) - \omega^2 M = 0$ is then solved with complex matrix $\tilde{L}$. Solutions are the complex set of eigenvalues $\left\{\tilde{\lambda}_0^{(m,n)}, \tilde{\lambda}_1^{(m,n)}, .., \tilde{\lambda}_k^{(m,n)}\right\}$.

- The second iteration provides better estimate for materials with frequency-dependent damping and elastic coefficients. The equivalent DLF of the assembly is finally computed from the band-averaged imaginary part of each complex eigenfrequencies.

5. VALIDATION

5.1 Modeling an aerospace structure (Case C1)

Case C1 is a 1 m x 1 m plate made of sandwich construction with two 1 mm-aluminum skins and 10 mm-core made of aluminum honeycomb with G = 2E8 Pa, E = 3E6 Pa, ρ_c = 60 kg/m^3.

SEA+ calculation is compared with two FEM simulations built for NASTRAN NX solver.

- C1 "PSOLID" FEM model, skins are modeled using 2D-plate elements and glued to the core meshed with 3D-solid elastic elements,
- C1 "PCOMP" FEM model, both skins and core are modeled with 2D PCOMP laminate elements within a single 2D-plate.

Real eigenmodes are extracted from both models by FEM solver and imported in SEA+ Virtual SEA solver [1] [2] [3] [4] to calculate related SEA parameters: modal density, wavenumber and mean input mobility. Post-processed SEA parameters of FEM models are then compared to SEA+ analytical Dynamic Laminate model. Figure 4 shows good agreement between SEA and FEM models.

The mid to high frequency slope of both flexural modal density and mobility spectra due to core shear is well-reproduced by SEA model. Shifting from PCOMP to PSOLID FEM models increases the first resonance frequencies. This is observed in the two selected boundary conditions: constraining one skin, then, two skins to simply-supported on edge, demonstrating the difficulty in predicting deterministic resonance frequencies even on simple systems.

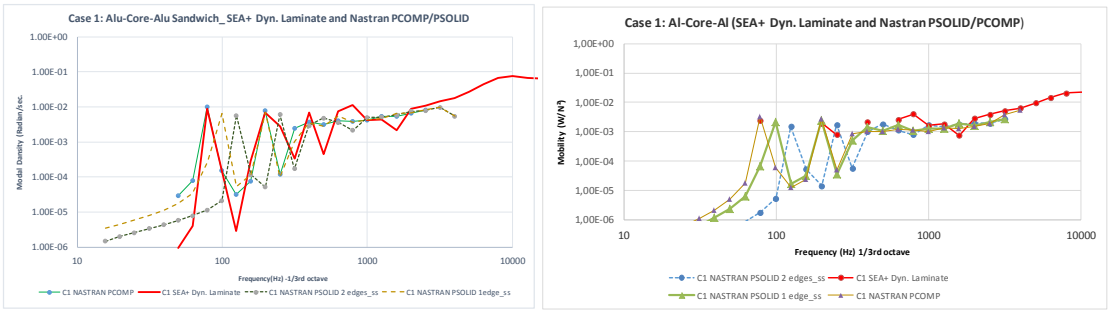

Figure 4 - Case C1 validation: Left, modal density and right, driving-point conductance (input mobility) for resp. for SEA and FEM models (PSOLID & PCOMP)

5.2 Modeling a thin steel sandwich (Case C2)

Case C2 is still a 3-layered sandwich made of two 1 mm-steel skins separated by a 1 mm-thick resilient material with E= 2.6E+07 Pa, G = 1E+07 Pa, ρ_v =1400 kg/m^3. Validation protocol is similar to previous case: the SEA model is compared to related FEM NASTRAN PCOMP and PSOLID models (resp. C2 “PCOMP” and C2-“PSOLID” FEM models). Figure 5 shows PCOMP model collapses above 1600 Hz with large over-prediction compared to PSOLID model results. PCOMP formulation based on zig-zag theory is only a valid formulation at low frequency. PCOMP model is unable in this case to fit with the physical behavior in principle better represented by PSOLID model. SEA+ formulation matches very accurately PSOLID results up to 300 Hz. Above some slight increase of modal density and mobility is seen due to softness of internal layer. PSOLID result is questionable at high frequency as mesh size was tuned to fit the criterion of 1/6 of the wavelength of the standalone skin below 3000 Hz and is then inappropriate for the core.

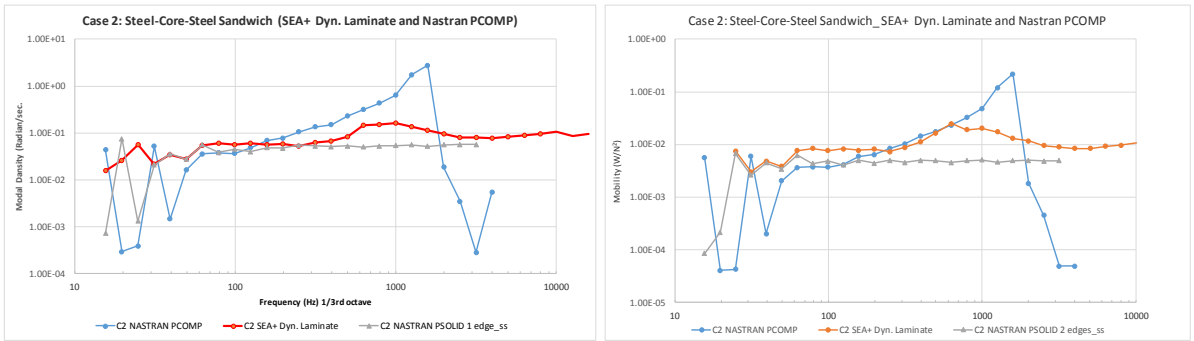

Figure 5 - Case C2 validation: Left, modal density and right, driving-point conductance (input mobility) for resp. for SEA and FEM models (PSOLID & PCOMP)

A correct mesh size based on the core wavelength would have made PSOLID model impossible to

solve. As seen in Figure 5, the Dynamic Laminate theory is matching with FEM results for the first modes then gives an intermediate result between PCOMP and PSOLID models with more robustness at high frequency where modal density is expected to converge to uncouple skin one with flat spectrum.

5.3 Modeling damped steel plate (Case C3)

Case C3 is also a 3-layered steel panel with very thin film of viscoelastic material bonding together two thin steel plates. Two similar samples of this kind from two manufacturers (Trelleborg and ThyssenKrupp) have been measured to compare with prediction arising from the various models. Characteristic used in the modeling are reported in next Table 1.

Table 1 - Characteristic of tested samples

Manufacturer	Panel size	Skin thickness	Core thickness	Core Young's modulus	Shear modulus	DLF core	Skin Mat.
Trelleborg	0.3m x 0.2m	0.8 mm	0.04 mm	50 MPa	40 MPa	1	Steel
ThyssenKrupp	0.275m x .2m	0.75 mm	0.04 mm	50 MPa	40 MPa	1	Steel

Measurements on both panels were given very similar results, hence core data estimated from Trelleborg data sheet were used to model ThyssenKrupp sandwich by Dynamic Laminate theory and by PCOMP and PSOLID models.

Core material intrinsic DLF is taken equal to 1. Skin DLF are fixed arbitrarily to 0.01.

Regarding measured data, a set of complex frequency transfer inertances were recorded under impact hammer for both test panels as well as driving point inertances converted into injected power per unit force per 1/3rd octave band. Reverberation time on free-free panels are also recorded and converted into DLF.

FEM models were only created for the ThyssenKrupp configuration. SEA models were made for both ThyssenKrupp and Trelleborg panels.

Mean DLF of PSOLID model is processed from synthesized numerical FRF by reverberation time analysis of the predicted impulse response obtained by inverse Fourier's transform.

In Figure 6 are reported calculated flexural modal densities and input conductances (including measurement) for the ThyssenKrupp panel. SEA+ modal density is very well fitted to both PCOMP and PSOLID results. For conductance, SEA result is best fitted to PSOLID model but PCOMP spectrum is not too different from other calculations above 400 Hz. SEA equivalent plate result is also given and is nearer from measured conductance. All Dynamic Laminate, PSOLID and PCOMP models seem then to over-predict by around 2 dB the measured conductance which seems not "feeling" any change in stiffness introduced by the thin film (closer to equivalent plate conductance).

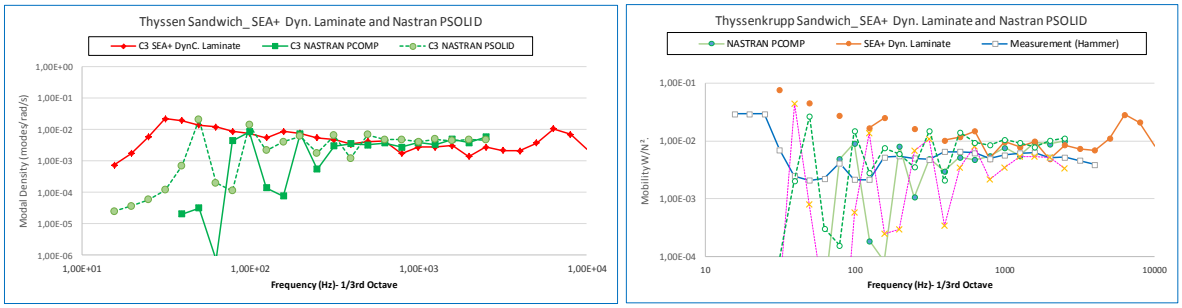

Figure 6 - Case C3 validation (ThyssenKrupp panel): Left, Flexural modal densities of SEA+ and Nastran (PCOMP and PSOLID), Right, normal driving-point conductance for resp. for SEA+ laminate and equivalent plate, PSOLID & PCOMP and measured data

SEA damping prediction (assuming 1%; 100%, 1% DLF distribution constant with frequency in the three layers) is given in Figure 7 compared to the measurement and to PSOLID prediction. The match between SEA and measured DLF is more representative than PSOLID model. Oddly, the latter under-predicts DLF for as much as 10 dB with same DLF layer-distribution. The core mesh is probably the cause of discrepancy, because the solid elements are 10 mm width with a thickness of only 0.05 mm and are certainly not representative of actual core behavior. Improving this ratio may be a rather difficult task due to necessary refinement of the mesh up to unbearable FEM model size. There is no

PCOMP DLF result as the NASTRAN PCOMP property only accepts one mean DLF value for all PCOMP sublayups.

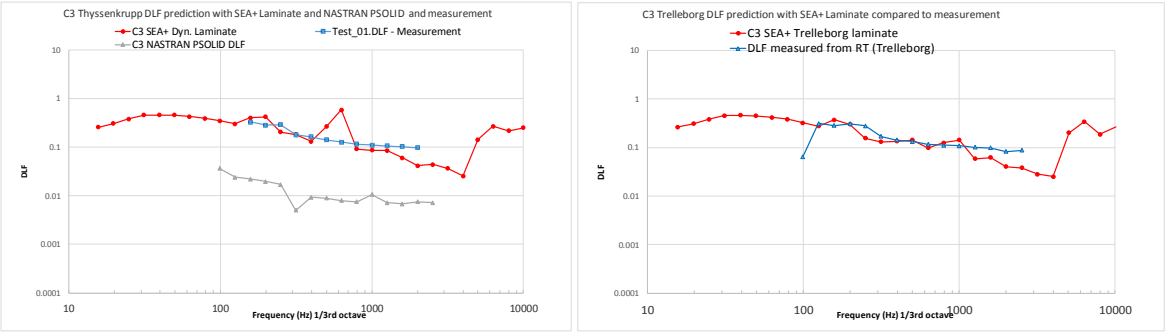

Figure 7 - Case C3 : Left ThyssenKrupp panel; simulated (Dynamic Laminate, PSOLID) and measured DLF; Right Trelleborg panel, simulated (Dynamic Laminate) and measured DLF

6. CONCLUSIONS

A new type of subsystem (Dynamic Laminate) has been created in SEA+ software based on an original multi-scaled laminate theory taking into account global and relative displacements of the layup internal layers. Analytical modes of the laminate subsystem are solved to derive relevant SEA parameters as well as mean damping loss factor from individual layers. The theory is still in validation process. Presented test cases have been first restricted to plate-like behavior and are demonstrating the validity of this approach providing in several circumstances better results than FEM prediction. Further work will follow with validation of singly-curved and doubly-curved formulations with or without stiffeners as well as thin acoustic cavities insertion.

ACKNOWLEDGEMENTS

The author acknowledges his coauthor in advance to deliver further test material to extend the validation to acoustic transmission loss prediction.

REFERENCES

1. G. Borello (InterAC), L. Gagliardini, L. Houillon (PSA), L. Petrinelli (Geci Systems),Virtual SEA: mid-frequency structure-borne noise modeling based on Finite Element Analysis, SAE Noise and Vibration Conference – May 6-8, 2003 – Traverse City, Michigan, USA
2. G. Borello, A. Courjal, R. Nguyen Van Lan (InterAC), Combining Finite Element and SEA approach in Vibroacoustic Analysis, 7th French Acoustic Congress – March 22-25, 2004 – Strasbourg, France
3. G. Borello (InterAC), L. Gagliardini, L. Houillon (PSA), L. Petrinelli (Geci Systems), Virtual SEA-FEA-based Modeling of Structure-Borne Noise, Sound and Vibration Magazine – January 2005
4. Analysing structure borne sound transmission in car body using combined FE/SEA techniques, G. Borello, A. Courjal, R. Nguyen Van Lan (InterAC), SIAT – January 19–22, 2005 – Pune, India
5. Borello (InterAC), J.-L. Kouyoumji (CTBA),Vibroacoustic Analysis of Sound Transmission in Double-glass Timber Windows, Inter-Noise – August 7-10, 2005 – Rio de Janeiro, Brazil
6. Luciano Demasi (San Diego University), An invariant Model for any Composite Plate Theory and FEM Applications: the Generalized Unified Formulation, 50th AIAA/ASME/ASCE/AHS/ASC Structures, Structural Dynamics and Material Conference 17th 4-7 May 2009, Palm Springs, CA, USA
7. Berthelot J.-M., Matériaux Composites, comportement mécanique et analyse des structures, Masson 2ème édition, 1996